



# $\beta$ 1 and $\beta$ 3 subunits amplify mechanosensitivity of the cardiac voltage-gated sodium channel Nav1.5

Michele Maroni<sup>1,2</sup> · Jannis Körner<sup>3,4</sup> · Jürgen Schüttler<sup>1</sup> · Beate Winner<sup>2</sup> · Angelika Lampert<sup>3</sup> · Esther Eberhardt<sup>1</sup>

Received: 25 May 2019 / Revised: 25 September 2019 / Accepted: 21 October 2019  
© Springer-Verlag GmbH Germany, part of Springer Nature 2019

## Abstract

In cardiomyocytes, electrical activity is coupled to cellular contraction, thus exposing all proteins expressed in the sarcolemma to mechanical stress. The voltage-gated sodium channel Nav1.5 is the main contributor to the rising phase of the action potential in the heart. There is growing evidence that gating and kinetics of Nav1.5 are modulated by mechanical forces and pathogenic variants that affect mechanosensitivity have been linked to arrhythmias. Recently, the sodium channel  $\beta$ 1 subunit has been described to stabilise gating against mechanical stress of Nav1.7 expressed in neurons. Here, we tested the effect of  $\beta$ 1 and  $\beta$ 3 subunits on mechanosensitivity of the cardiac Nav1.5.  $\beta$ 1 amplifies stress-induced shifts of  $V_{1/2}$  of steady-state fast inactivation to hyperpolarised potentials ( $\Delta V_{1/2}$ : 6.2 mV without and 10.7 mV with  $\beta$ 1 co-expression).  $\beta$ 3, on the other hand, almost doubles stress-induced speeding of time to sodium current transient peak ( $\Delta$ time to peak at  $-30$  mV: 0.19 ms without and 0.37 ms with  $\beta$ 3 co-expression). Our findings may indicate that in cardiomyocytes, the interdependence of electrical activity and contraction is used as a means of fine tuning cardiac sodium channel function, allowing quicker but more strongly inactivating sodium currents under conditions of increased mechanical stress. This regulation may help to shorten action potential duration during tachycardia, to prevent re-entry phenomena and thus arrhythmias.

**Keywords** Sodium channel · Mechanosensitivity · Patch-clamp · Cardiac ion channel

## Introduction

Voltage-gated sodium channels are essential for the generation and propagation of action potentials in excitable tissues. They are macromolecular complexes that consist of a pore forming  $\alpha$  subunit and regulatory  $\beta$  subunits [7, 8].  $\alpha$  subunits are large (260 kDa) proteins that contain four homologous domains (DI-

DIV) of six transmembrane segments (S1-S6) that include a voltage sensing domain (VSD, S1-4) and a pore domain (S5-6). In contrast,  $\beta$  subunits are small proteins (30–40 kDa) with one transmembrane domain and are either linked to the  $\alpha$  subunit via a disulphide bridge or are non-covalently bound [6, 33]. In humans, nine Navs (Nav1.1–Nav1.9) and four  $\beta$  subunits ( $\beta$ 1– $\beta$ 4) are known to date. Their concerted interaction is crucial for channel gating and surface expression. Mutations in both  $\alpha$  and  $\beta$  subunits as well as  $\beta$  subunit deficiency in mice lead to severe disorders due to altered excitability like epilepsy syndromes, pain, and arrhythmias [10, 13, 25, 46].

Besides regulation by accessory proteins, Navs themselves have been found to be mechanosensitive [32, 38, 40]. In neurons, especially in the peripheral nervous system, action potentials need to initiate and propagate independently of mechanical stress induced by, e.g., body movement. Recently,  $\beta$ 1 has been shown to stabilise the neuronal Nav1.7 against mechanical stress [17]. The non-covalently bound  $\beta$  subunits  $\beta$ 1 and  $\beta$ 3 share most homology among all isoforms and have been implicated in cardiac conduction diseases like Brugada Syndrome or atrial or ventricular fibrillation [5, 11, 14, 26, 41, 42]. In the heart, each action potential is followed by a cellular

**Electronic supplementary material** The online version of this article (<https://doi.org/10.1007/s00424-019-02324-w>) contains supplementary material, which is available to authorized users.

✉ Esther Eberhardt  
esther.eberhardt@uk-erlangen.de

- <sup>1</sup> Department of Anaesthesiology, Friedrich-Alexander-Universität Erlangen-Nürnberg (FAU), 91054 Erlangen, Germany
- <sup>2</sup> Department of Stem Cell Biology, Friedrich-Alexander-Universität Erlangen-Nürnberg (FAU), 91054 Erlangen, Germany
- <sup>3</sup> Institute of Physiology, Medical Faculty, RWTH Aachen University, 52074 Aachen, Germany
- <sup>4</sup> Department of Anaesthesiology, Medical Faculty, RWTH Aachen University, 52074 Aachen, Germany

contraction, thus mechanical stress of the proteins expressed in the sarcolemma occurs inherently under physiological conditions. It has been shown that especially Nav1.5, the predominant cardiac isoform [7, 16] is regulated by various mechanical stimuli in a partly reversible and dose-dependent manner [2, 22]. Regulation of Nav1.5 by mechanical stress can contribute to the mechano-electric feedback, which is important for normal cardiac function and the pathophysiology of arrhythmogenesis [21, 28], but its molecular mechanisms are incompletely understood. A potential involvement of  $\beta 1$  and  $\beta 3$  in the regulation of mechanosensitivity of Nav1.5 is therefore likely but has not been investigated so far.

In the present study, we analysed how heterologous co-expression of  $\beta 1$  and  $\beta 3$  subunits with Nav1.5 affects mechano-induced changes in gating and kinetics. Unlike the stabilising effect of  $\beta 1$  on activation and inactivation of Nav1.7 under mechanical stress [17],  $\beta 1$  amplifies mechano-induced shifts in inactivation of Nav1.5. In contrast,  $\beta 3$  does not alter changes of the voltage sensitivity under mechanical stimulation but enhances mechano-induced speeding of gating kinetics. Our results suggest that mechanosensitivity of Nav1.5 is differentially regulated by  $\beta 1$  and  $\beta 3$  and that the mechanomodulative role of  $\beta$  subunits is dependent on the interacting Nav. Therefore,  $\beta$  subunits provide a molecular mechanism to fine tune Nav-activity and thereby adapt cellular excitability to acutely altered mechanical forces much quicker than mechanisms of transcriptional regulation.

## Materials and methods

### Cell culture and transfection

HEK293 cells were maintained in IMDM with 10% FBS and 1% Pen/Strep (all Life Technologies) at 37 °C and 5% CO<sub>2</sub>. Constructs containing hNav1.5 in a modified pTracer vector, GFP (Lonza), or modified pCLH vectors containing either human  $\beta 1$  with a pIRES site for GFP or a c-terminally GFP-tagged human  $\beta 3$  were used for co-expression experiments. For transfection, PEI max 40K (Polysciences Inc.) was diluted according to the manufacturer's instructions to a concentration of 1 mg/mL. Four microliters of the dilution was added to 200  $\mu$ L OptiMEM (Life Technologies) and mixed with plasmids of hNav1.5 (1  $\mu$ g) with either 0.3  $\mu$ g of GFP, h $\beta 1$ , or h $\beta 3$ -GFP containing vectors in 200  $\mu$ L OptiMEM and incubated for 20 min at room temperature. Several studies used similar GFP-tagged constructs and reported functional preservation of  $\beta$  subunit properties by direct comparison of fluorescently tagged and untagged constructs [18, 48]. However, we cannot fully exclude an impact on mechanosensitivity of the GFP-tagged  $\beta 3$  construct. Cells were kept in antibiotic-free media for transfection and incubated 24–28 h before experiments.

### Electrophysiology

All recordings were made with a HEKA EPC10 USB system at room temperature. Glass pipettes (tip resistance 1.0–2.5 M $\Omega$ ) were manufactured with a DMZ puller (Zeitz Instruments GmbH) and filled with internal solution containing (in mM): 140 CsF, 2 NaCl, 10 Hepes, 1 EGTA, 15 glucose (pH 7.33, adjusted with CsOH). The bath solution contained (in mM) 70 CholineCl, 70 NaCl, 3 KCl, 1 MgCl<sub>2</sub>, 1 CaCl<sub>2</sub>, 10 Hepes, 20 glucose (pH 7.4, adjusted with NaOH). Capacitive transients were cancelled online during gigaseal formation, series resistance was compensated to 75% and cells having series resistance > 5 M $\Omega$  were excluded from analysis. Mechanical stress was applied as shear stress with a gravity-driven perfusion pencil (Automate Scientific 4 channel perfusion pencil, tip: internal diameter 360  $\mu$ m) positioned at 1100  $\mu$ m from the cell. The flow was set to approximately 300  $\mu$ L/min (tip flow: 41.4 cm/s) and was initiated before establishing whole-cell configuration. To correct for time-dependent changes in gating, each condition (Nav1.5, Nav1.5 +  $\beta 1$  or  $\beta 3$ ) was either recorded with or without mechanical stimulation in a time-matched experimental approach. Traces were acquired at a 100 kHz frequency and low-pass filtered at 2.83 kHz. Leak correction was performed online using the P/4 method with alternate leak pulses recorded after the test pulse. Prior to recordings, cells were equilibrated for 3 min at a holding potential of –120 mV.

Current-voltage relations were obtained by 10 mV voltage steps of 100 ms ranging from –100 to +30 mV at an interval of 10 s. The conductance of voltage-dependent sodium currents ( $G_{Na}$ ) was calculated using the following equation:  $G_{Na} = I_{Na} / (V_{mem} - E_{rev})$ .  $I_{Na}$  is the current at the voltage  $V_{mem}$ ,  $E_{rev}$  is the reversal potential for sodium that was calculated for each cell individually and normalised conductance ( $G/G_{max}$ ) was plotted versus test voltage. Voltage of half maximal activation ( $V_{1/2}$ ) and the slope factor ( $k$ ) were calculated by fitting the function with the Boltzmann equation  $G(V_{mem})/G_{max} = 1 / (1 + e^{(V_{mem} - V_{1/2})/k})$ .

Voltage dependence of steady-state fast inactivation was recorded by a series of 500 ms pre-pulses from –180 to –20 mV in 10 mV steps each followed by a 40 ms depolarisation to 0 mV (test pulse) to record currents of non-inactivated channels. Peak inward sodium currents at each test pulse were normalised to the maximal inward current ( $I/I_{max}$ ), plotted versus pre-pulse voltage, and fitted by the Boltzmann function  $I(V_{mem})/I_{max} = 1 / (1 + e^{(V_{mem} - V_{1/2})/k})$  to calculate the half maximal potential ( $V_{1/2}$ ) and slope factor ( $k$ ) of inactivation.

Time to peak was calculated as time required by the current from onset of depolarisation to reach its maximum at potentials between –50 mV and 30 mV in the activation protocol.

Time constants of inactivation were obtained by fitting the decay of Nav currents with a biexponential function using Igor Pro 5.0.2.0.

## Data analysis and statistics

Data were analysed using the Fitmaster software (HEKA), Excel (Microsoft Corporation) with the Real Statistics Resource Pack software plugin v5.2 (Zaiontz C., 2018, [www.real-statistics.com](http://www.real-statistics.com)), Origin 9.1 (Origin Lab), and Igor Pro 5.0.2.0 (Wavemetrics). Plots were made with Prism 6.2 (Graphpad Software), Inkscape 0.92.3 (GPL software), and Corel Draw X6 (Corel Corporation). Data are presented as mean  $\pm$  SEM unless stated otherwise. Each group contains experiments of at least three different transfections. All groups were analysed by D'Agostino-Pearson test to assess normality distribution of underlying data points. Consequently one-way ANOVA with Tukey's post hoc test was used for normally distributed data and a Kruskal-Wallis test followed by Dunn's multiple comparison test was used for non-parametric testing.  $p$  values  $< 0.05$  were considered significant and are indicated as follows: \* $p < 0.05$ ; \*\* $p < 0.01$ ; \*\*\* $p < 0.001$ . For means of clarity, levels of significance are only given for comparisons that illustrate either the effects of mechanical stress or  $\beta$  subunits.

## Homology modelling

The 4.0 Å cryo-EM structure of the electric eel Nav1.4- $\beta$ 1 complex (PDB ID 5XSY) [45] provided the structural template for construction of a hNav1.5-h $\beta$ 1 or hNav1.5-h $\beta$ 3 complex homology model. Sequence alignment was performed using Jalview [44] and 100 loop-refined models were generated with MODELLER 9.19 [31]. The best model was chosen based on the implemented DOPE-HR score in MODELLER and visual inspection.

## Results

### Half maximal voltage of activation of Nav1.5 is unchanged by $\beta$ 1 co-expression or mechanical stress

To investigate mechanosensitivity of Nav1.5 in dependence of the  $\beta$ 1 and  $\beta$ 3 subunit, we used a standardised bath flow to induce mechanical stress on transiently transfected HEK293 cells. Current density in cells expressing Nav1.5 remained unchanged by co-expression of  $\beta$ 1 and was also unaffected by mechanical stimulation ( $-308.8 \pm 33.81$  pA/pF, Fig. 1, Table 1). Consistent with previously published results for bath flow as mechanical stimulus [4], we did not observe any impact on the midpoint ( $V_{1/2}$ ) of activation of Nav1.5 (Fig. 1).  $V_{1/2}$  of activation was  $-41.6 \pm 0.7$  mV for Nav1.5 alone and was also unaffected by co-expression of  $\beta$ 1 (Fig. 1b, c).

Solely, the slope of activation was slightly but significantly less steep under mechanical stimulation in the presence of  $\beta$ 1 (see Table 1 for summary).

### $\beta$ 3 co-expression shifts activation of Nav1.5 to depolarised potentials

In contrast to  $\beta$ 1,  $\beta$ 3 depolarised  $V_{1/2}$  of activation of Nav1.5 by 5.9 mV (Fig. 2). Also, under mechanical stress, the depolarisation of activation of Nav1.5 by  $\beta$ 3 was retained (Fig. 2b, c). There was a small but significant effect on the slope factor of activation that mirrored the findings found for  $V_{1/2}$  of activation in all groups as  $\beta$ 3 increased the slope factor of activation independent of mechanical stimulation (for summary see Table 1).

### $\beta$ 1 amplifies mechanosensitivity of Nav1.5 steady-state fast inactivation

Co-expression of  $\beta$ 1 with Nav1.5 led to a depolarisation of inactivation by 5.4 mV and the slope was observed to be steeper in the presence of  $\beta$ 1. In accordance with previous results for negative pressure [2, 3], mechanical stress resulted in pronounced hyperpolarisation of  $V_{1/2}$  of steady-state fast inactivation of Nav1.5 by 6.2 mV (Fig. 3). In contrast to its effects on the neuronal subtype Nav1.7 [17], we did not observe a mechano-protective effect of  $\beta$ 1 co-expression on inactivation of the cardiac isoform Nav1.5. On the contrary,  $\beta$ 1 seems to amplify the mechano-induced shift of inactivation from a  $\Delta V_{1/2}$  of 6.2 mV without  $\beta$ 1 to a  $\Delta V_{1/2}$  of 10.7 mV with  $\beta$ 1 (Fig. 3, Table 1). As observed for activation, the slope was less steep in the presence of  $\beta$ 1 under mechanical stimulation. Thus, mechanical stress can regulate Nav1.5 inactivation among a larger range of voltages when  $\beta$ 1 is co-expressed.

Similar to  $\beta$ 1, co-expression of  $\beta$ 3 with Nav1.5 induced a notable depolarising shift in the voltage dependence of steady-state inactivation ( $\Delta V_{1/2}$  6.4 mV). Mechanical stimulation equally hyperpolarised inactivation of Nav1.5 alone or co-expressed with  $\beta$ 3 by 6.2 mV and 7.5 mV, respectively (Fig. 4a, b), suggesting only a moderate amplification of the stress-induced shift of  $V_{1/2}$  compared to  $\beta$ 1 (Table 1).

### $\beta$ 3 enhances mechanical induced speeding of gating kinetics of Nav1.5.

It was previously reported that mechanical stress not only affects the voltage-dependence of activation and inactivation but also their kinetics [2, 4, 35]. As current traces were indicative for such changes (Figs. 1a and 2a and Supplementary Fig. 1), we used time to peak as a measure for activation kinetics. We found that in contrast to  $\beta$ 1,  $\beta$ 3 delayed time to peak of Nav1.5 in control conditions over the whole voltage range (Fig. 5c). Mechanical stress speeds up channel

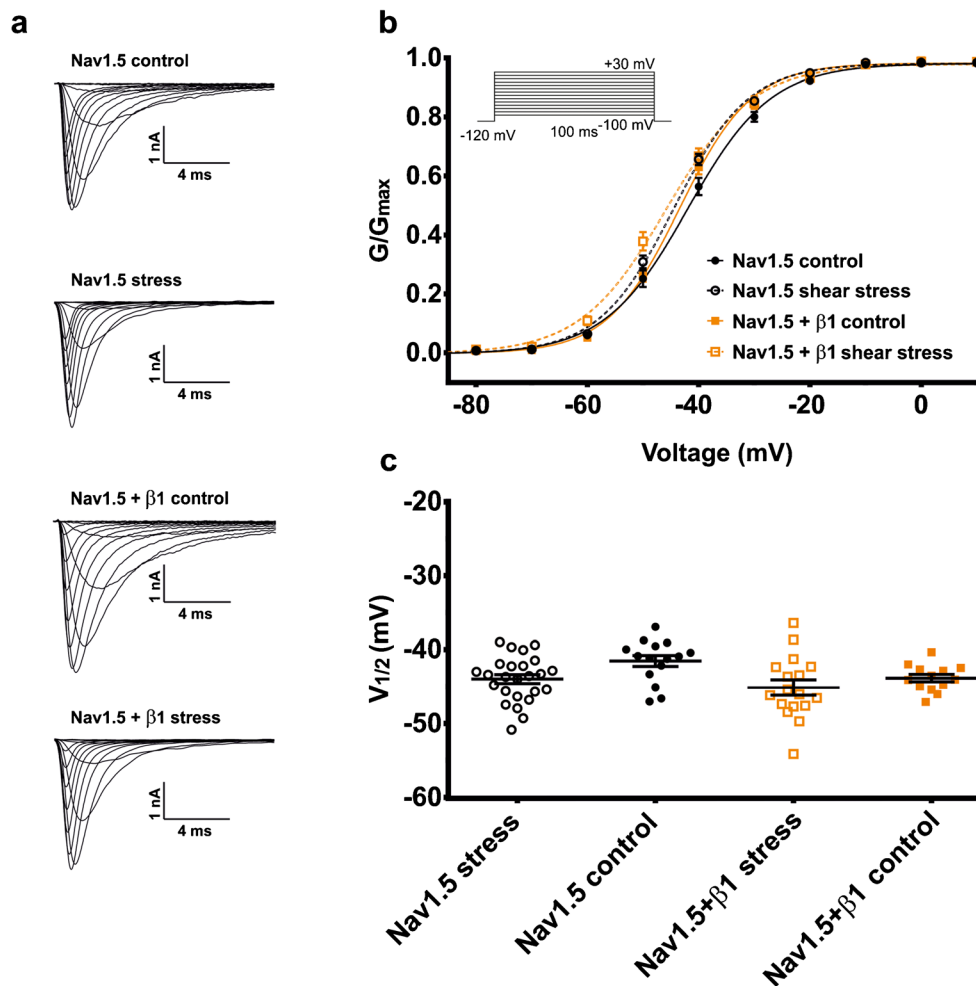


**Fig. 1** Half maximal voltage of activation of Nav1.5 is not changed by mechanical stress nor by co-expression of the  $\beta 1$  subunit. HEK293 cells transiently transfected with Nav1.5 and Nav1.5 +  $\beta 1$  subunit were recorded with or without (flow-induced) mechanical stress. **a** Representative sodium current traces of Nav1.5 and Nav1.5 +  $\beta 1$  without and with mechanical stress elicited by the voltage protocol given in the inset of **b**. **b** Conductance-voltage plots fitted with a Boltzmann function and **c** derived half maximal voltage of activation ( $V_{1/2}$ ) for individual experiments.  $V_{1/2}$  is displayed as mean  $\pm$  SEM

activation under all conditions measured and reached significance for Nav1.5 alone and in co-expression with  $\beta 3$  (Fig. 5). Notably, stress-induced delta of time to peak at  $-30$  mV was nearly doubled by co-expression of  $\beta 3$ , from a speeding of 0.19 ms under control conditions, to 0.37 ms when  $\beta 3$  was present (Fig. 5c, d, Table 1).

Inactivation of Nav1.5 was well described by a biexponential function resulting in a fast ( $\tau_{1}$ ) and a slow time constant ( $\tau_{2}$ ) that accounted for the average of  $82 \pm 1.1\%$  and  $17.9 \pm 1.0\%$  percent of the current for all groups. For Nav1.5,  $\tau_{1}$  was  $1.09 \pm 0.04$  ms and  $\tau_{2}$  was  $6.24 \pm 0.37$  ms and both time constants were significantly accelerated by mechanical stress. Similar to the findings for activation kinetics, the co-expression of the  $\beta 3$  subunit enhanced mechano-induced acceleration of inactivation from a  $\Delta\tau_{1}$  of 0.4 ms

with individual data points and was not significantly affected by mechanical stress or co-expression of  $\beta 1$ .  $V_{1/2}$  of activation for Nav1.5 control was  $-41.6 \pm 0.7$  mV (filled black circles,  $n = 15$ ) and  $-43.9 \pm 0.5$  mV for Nav1.5 +  $\beta 1$  control (filled orange squares,  $n = 13$ ). With mechanical stress  $V_{1/2}$  of activation of Nav1.5 was  $-44.0 \pm 0.6$  mV (Nav1.5 shear stress, open black circles,  $n = 25$ ) and  $-45.1 \pm 1.0$  mV for Nav1.5 co-expressed with  $\beta 1$  (Nav1.5 +  $\beta 1$  shear stress, open orange squares,  $n = 17$ ; one-way ANOVA with Tukey's multiple comparison test)

for Nav1.5 alone to 0.69 ms whereas in the presence of  $\beta 1$ , inactivation kinetics remained unchanged by mechanical stimulation (Table 1, Supplementary Figs. 1 and 2)

Thus, co-expression of  $\beta 3$  offers a larger working range for mechanically induced changes, which allows for speeding and slowing of time to peak (and thus potentially alteration of the slope of the action potential), depending on the intensity of mechanical stress in the cardiomyocyte.

### Homology modelling suggests different affinity of non-covalently bound $\beta$ subunits to the putative binding site in Nav1.5

Differences in mechanomodulation of Nav1.5 by  $\beta$  subunits could arise in the binding to distinct and/or multiple binding

**Table 1** Properties of Nav1.5 currents in dependence of co-expression of  $\beta 1$  or  $\beta 3$  and mechanical stimulation

	Nav1.5	Nav1.5 stress	Nav1.5 $\beta 1$	Nav1.5 $\beta 1$ stress	Nav1.5 $\beta 3$	Nav1.5 $\beta 3$ stress
<b>Activation</b>						
$V_{1/2}$ (mV)	$-41.6 \pm 0.7$	$-44.0 \pm 0.6$	$-43.9 \pm 0.5$	$-45.1 \pm 1.0$	$-35.7 \pm 1.2^{§§}$	$-37.2 \pm 1.4^{§§§}$
Slope (1/mV)	$7.2 \pm 0.2$	$6.8 \pm 0.2$	$6.3 \pm 0.3$	$7.7 \pm 0.3^{**}$	$8.5 \pm 0.2^{§§}$	$8.7 \pm 0.2^{§§§}$
$\Delta V_{1/2}$	2.4		1.2		1.5	
Time to peak at $-30$ mV (ms)	$0.97 \pm 0.03$	$0.78 \pm 0.02^{***}$	$0.97 \pm 0.02$	$0.85 \pm 0.03$	$1.17 \pm 0.05$	$0.8 \pm 0.03^{***}$
$\Delta$ time to peak (ms)	0.19		0.12		0.37	
$\tau_{1}$ at $-30$ mV (ms)	$1.09 \pm 0.04$	$0.69 \pm 0.06^{***}$	$0.98 \pm 0.06$	$0.91 \pm 0.1$	$1.51 \pm 0.12$	$0.82 \pm 0.07^{***}$
$\Delta \tau_{1}$ (ms)	0.4		0.07		0.69	
Amp1 (%)	$85.4 \pm 1.3$	$83.0 \pm 2.5$	$84.3 \pm 2.6$	$78.2 \pm 2.8$	$80.1 \pm 3.4$	$81.4 \pm 2.0$
$\tau_{2}$ at $-30$ mV (ms)	$6.24 \pm 0.37$	$4.14 \pm 0.35^{*}$	$5.97 \pm 0.76$	$7.02 \pm 0.95$	$8.2 \pm 1.36$	$5.7 \pm 0.6$
Amp2 (%)	$14.6 \pm 1.4$	$16.8 \pm 2.4$	$14.7 \pm 2.2$	$21.4 \pm 2.6$	$19.6 \pm 3.2$	$19.9 \pm 2.4$
Current density	$-308.8 \pm 33.8$	$-365.8 \pm 41.0$	$-522.9 \pm 114$	$-339.2 \pm 31.3$	$-297.1 \pm 37.6$	$-234.1 \pm 23.4$
<b>Inactivation</b>						
$V_{1/2}$ (mV)	$-99.0 \pm 0.9$	$-105.2 \pm 0.9^{**}$	$-93.6 \pm 0.6^{§}$	$-104.3 \pm 1.9^{***}$	$-92.6 \pm 1.4^{§§}$	$-100.1 \pm 1.2^{§,***}$
Slope (1/mV)	$6.0 \pm 0.1$	$6.1 \pm 0.1$	$4.9 \pm 0.1^{§§}$	$6.3 \pm 0.3^{***}$	$5.4 \pm 0.1$	$6.2 \pm 0.3$
$\Delta V_{1/2}$	6.2		10.7		7.5	

Significance levels are given for comparisons of mechanical stress to control conditions indicated by \* and for the effects of the  $\beta 1$  or  $\beta 3$  subunits compared to Nav1.5 indicated by  $§$  ( $*/§ p < 0.05$ ;  $**/§§ p < 0.01$ ,  $***/§§§ p < 0.001$ ).  $\Delta$ : difference in the means between control condition and mechanical stress for each group

sites as well as variability in the interaction at the same binding site. Functional studies suggested different interactions and mechanisms of gating modulation for non-covalently bound  $\beta$  subunits and Nav1.5 [47]. However, no structural data is available for the interaction of Nav1.5 with any of the  $\beta$  subunits. We wondered what insights we could obtain using the resolved cryo-EM structure of the Nav1.4- $\beta 1$  complex [45] as a template for Nav1.5- $\beta 1/3$  interaction. This allowed us to compare the modelled binding interfaces of Nav1.5- $\beta 1$  and Nav1.5- $\beta 3$  at the proposed interaction site at VSDIII by analysing the distances between the side chains of the  $\alpha$  and  $\beta$  subunits. We define potential interacting sites as sidechains modelled within a distance of 3 Å to the other subunit (Fig. 6 and Supplementary table 1).  $\beta 3$  appears to possess a higher number of interactions with its extracellular domain (ECD) and the extracellular loops of Nav1.5 as well as with its transmembrane domain (TMD) bound to VSDIII. This may explain the more pronounced effects of  $\beta 3$  on channel activation kinetics. We observed that the interaction with the extracellular loops of Nav1.5 was not identical for both  $\beta$  subunits: they seem to be more pronounced at the extracellular parts of the loops between S5 and S6 in DIV and DI for  $\beta 3$  compared to  $\beta 1$ .

## Discussion

In this study, we characterise the effects of the  $\beta 1$  and  $\beta 3$  subunits on the mechanosensitivity of the cardiac sodium

channel Nav1.5. Our results show that both  $\beta$  subunits differentially regulate the mechanical susceptibility of this channel. In particular,  $\beta 1$  amplifies mechano-induced gating changes of inactivation whereas  $\beta 3$  mostly promotes speeding of gating kinetics.

In our experimental setting, we chose standardised bath flow as stimulus which was kept constant within the capabilities of this experimental setting and observed a reliable hyperpolarisation of inactivation of Nav1.5 ( $\Delta V_{1/2}$  6.2 mV) as a prerequisite to investigate the impact of  $\beta$  subunits on mechanosensitivity of Nav 1.5. However, changes in gating and kinetics of Navs induced by mechanical stimulation seem to be dependent on the magnitude and mode of the stimulus as well as the cellular background. The latter supports the idea that mechanosensitivity of voltage-gated channels seems to be regulated by proteins which expression vary between different tissues. So far shifts of activation and inactivation of Navs have not uniformly been reported but if they occur they are consistently found to be in the hyperpolarising direction [2, 4, 36] and a hyperpolarisation of inactivation has been also described for Nav1.6 [40], Nav1.4 [32], and Nav1.7 [17]. Mechano-induced effects on gating kinetics also vary among experimental settings but uniformly seem to be accelerated which also matches our observations [2, 37] The experimental setting of this study was designed to answer the question if  $\beta 1$  and  $\beta 3$  can influence mechanosensitivity of Nav1.5 in general but is not suited to draw conclusions about dose-dependency of shear stress and to apply higher more physiological flow rates. From what is known to date from using pressure clamp

**Fig. 2** Effects of  $\beta 3$  on activation of Nav1.5 remain unchanged under mechanical stress. **a** Representative sodium current traces from Nav1.5 and Nav1.5 +  $\beta 3$  expressed in HEK293 cells without and with mechanical stress elicited by the protocol given in **b**. **b** Boltzmann fits of voltage dependence of normalised sodium conductance. **c**  $V_{1/2}$  of activation presented as mean  $\pm$  SEM with single data points for Boltzmann fits of individual experiments. Co-expression of  $\beta 3$  caused a significant depolarisation of the  $V_{1/2}$  of activation in control conditions. Mean  $\pm$  SEM values were  $-41.6 \pm 0.7$  mV for Nav1.5 control (filled black circles,  $n = 15$ ),  $-35.7 \pm 1.2$  mV for Nav1.5 +  $\beta 3$  control (filled blue diamonds,  $n = 16$ ),  $-44.0 \pm 0.6$  mV for Nav1.5 + mechanical stress (open black circles,  $n = 25$ ) and  $-37.2 \pm 1.4$  mV for Nav1.5 +  $\beta 3$  + mechanical stress (open blue diamonds,  $n = 17$ ; one-way ANOVA with Tukey's multiple comparison test)

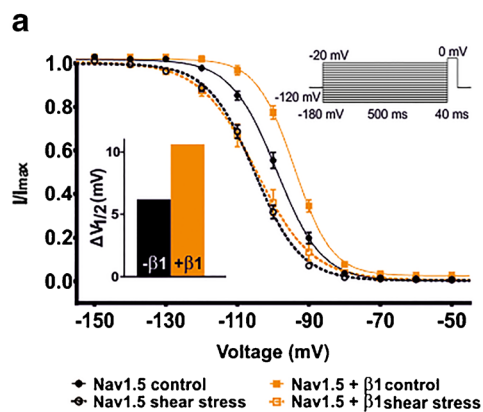
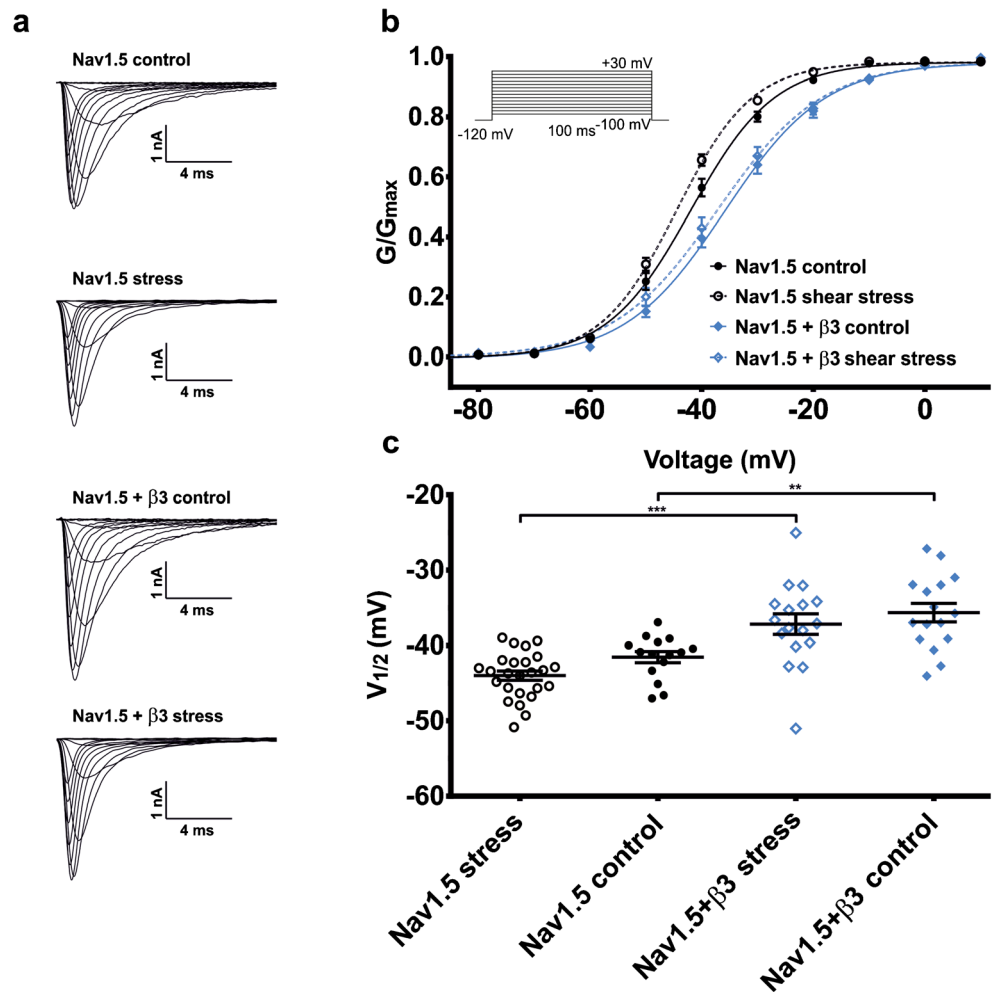
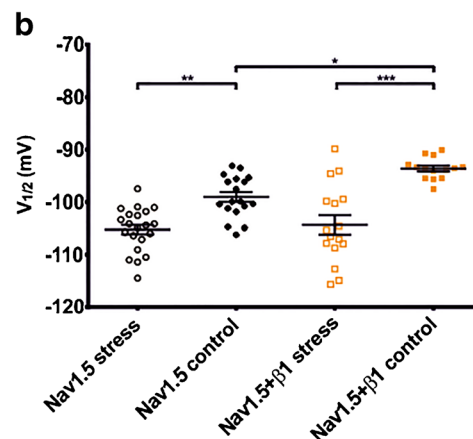


**Fig. 3**  $\beta 1$  expression amplifies mechano-induced changes in steady-state fast inactivation of Nav1.5. **a** Normalised currents showing voltage dependence of steady-state fast inactivation for Nav1.5 and Nav1.5 +  $\beta 1$  with and without mechanical stress. **b** Half maximal voltage of inactivation ( $V_{1/2}$ ) was calculated from Boltzmann fits of individual experiments and is depicted as mean  $\pm$  SEM with individual data points. The difference of  $V_{1/2}$  of inactivation ( $\Delta V_{1/2}$ ) for Nav1.5 alone or co-expressed with  $\beta 1$  between control condition and mechanical stress is given as a bar graph in the inset of **a**.  $\beta 1$  expression depolarised the  $V_{1/2}$



of inactivation of Nav1.5 by 5.4 mV. Mechanical stress caused a hyperpolarising shift in  $V_{1/2}$  of inactivation by 6.2 mV for Nav1.5 alone that was amplified by  $\beta 1$  expression to a  $\Delta V_{1/2}$  of 10.7 mV.  $V_{1/2}$  of inactivation was  $-99.0 \pm 0.9$  mV for Nav1.5 control (filled black circles,  $n = 18$ ) and  $-93.6 \pm 0.6$  mV for Nav1.5 +  $\beta 1$  control (filled orange squares,  $n = 14$ ). Under mechanical stress,  $V_{1/2}$  of inactivation was shifted to  $-105.2 \pm 0.9$  mV (Nav1.5 stress, open black circles,  $n = 21$ ) and to  $-104.3 \pm 1.9$  mV for Nav1.5 +  $\beta 1$  (Nav1.5 +  $\beta 1$  stress, open orange squares,  $n = 16$ ; one-way ANOVA with Tukey's multiple comparison test)

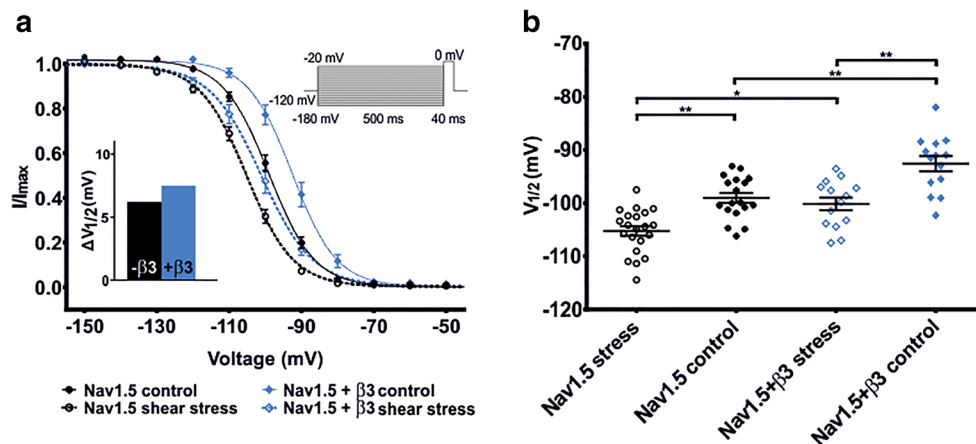


**Fig. 4**  $\beta 3$  does not affect mechanosensitivity of steady-state fast inactivation of Nav1.5. **a** Voltage dependence of steady-state fast inactivation for Nav1.5 (black circles) and Nav1.5 +  $\beta 3$  (blue diamonds) with (open symbols) and without mechanical stress (filled symbols). **b** Mean  $\pm$  SEM for  $V_{1/2}$  of inactivation obtained by Boltzmann fits for individual experiments.  $\beta 3$  expression depolarised  $V_{1/2}$  of inactivation by 6.4 mV. Mechanical stress equally

hyperpolarised  $V_{1/2}$  of inactivation for Nav1.5 alone and Nav1.5 +  $\beta 3$  by 6.2 mV and 7.5 mV respectively as depicted in the inset of **a**. Mean  $\pm$  SEM for  $V_{1/2}$  of inactivation were  $-99.0 \pm 0.9$  mV without (Nav1.5 control,  $n = 18$ ) and  $-92.6 \pm 1.4$  mV with  $\beta 3$  under control conditions (Nav1.5 +  $\beta 3$  control,  $n = 14$ ) and  $-105.2 \pm 0.9$  mV (Nav1.5 stress,  $n = 21$ ) and  $-100.1 \pm 1.2$  mV (Nav1.5 +  $\beta 3$  stress,  $n = 14$ ) under mechanical stress. One-way ANOVA with Tukey's multiple comparison test

as more quantitative method to apply force, Nav1.5 alone responds to mechanical stress in a dose-dependent manner [2]. Further work is needed to elucidate how  $\beta$  subunits add to this dynamic response and to previous findings of other mechanical stimuli.

The impact of the  $\beta 1$  subunit on mechanomodulation of Nav1.5 found in this study is distinct from previous observations with other Nav subtypes. Expression of  $\beta 1$  did not seem to alter the response of Nav1.6 to mechano-induced changes in gating and kinetics [40]. However, it has recently been shown that  $\beta 1$  stabilises gating of Nav1.7 against bath flow induced hyperpolarisation [17]. In accordance with previous observations in HEK cells,  $\beta 1$  caused a considerable depolarisation of inactivation [47]. Unlike to its effects on Nav1.7,  $\beta 1$  could not stabilise inactivation of Nav1.5 against mechanical stimulation but conversely amplified the mechano-induced hyperpolarisation of inactivation. These findings suggest that regulation of mechanosensitivity by the same isoform of  $\beta$  subunits might be dissimilar between different Nav isoforms.

To our knowledge, no previous study has addressed the regulation of mechanosensitivity of Navs by other  $\beta$  subunits than  $\beta 1$ . Here, we show that  $\beta 3$  depolarises  $V_{1/2}$  of activation and inactivation of Nav1.5 but unlike  $\beta 1$  does not seem to affect mechano-induced gating shifts of inactivation. However, we found that  $\beta 3$  is able to enhance acceleration of gating kinetics by mechanical forces. Therefore, our findings suggest that mechanomodulation is not only restricted to  $\beta 1$  but that distinct  $\beta$  subunits rather differentially regulate mechanosensitivity of Navs. Moreover, mechanomodulation by  $\beta$  subunits does not only affect voltage sensitivity but also seems to include gating kinetics.

It has previously been shown that mechanical stress stabilises inactivated states of Nav1.5 [2, 36], accelerates

spontaneous beating and also the decay slope of action potentials of atrial myocyte-derived HL1 cells [36]. As  $\beta 1$  seems to extend the voltage range among which mechanical stimulation can regulate inactivation of Nav1.5,  $\beta 1$  would potentiate this mechanisms. Stronger inactivation would limit late persistent sodium current during repolarization of the action potential thereby making early afterdepolarizations more unlikely [12, 20]. In addition, mechano-induced acceleration of activation by  $\beta 3$  would potentially alter the slope of the action potential and could lead to better sodium channel synchronisation, faster calcium channel opening and thus support  $\text{Ca}^{2+}$ -influx in the presence of stress. Our findings may indicate that in cardiomyocytes the inherent mechanical stress followed by each action potential is used as a means of fine tuning cardiac sodium channel function, allowing quicker activating but more strongly inactivating sodium currents under conditions of increased mechanical stress. This regulation allows a fast-acting adjustment process that may help to shorten action potential duration during tachycardia, to prevent re-entry phenomena and thus arrhythmias.

Navs differ in electrical properties and thus have distinct roles in action potential generation [8, 29]. As mechanosensitivity does not seem to be comparable among Nav isoforms and is moreover differentially regulated by  $\beta$  subunits, it is tempting to speculate that mechanical forces could not only influence the contribution of Navs to electromechanical coupling but also to electrogenesis.

Mechanisms that has been described to be important for mechanosensitivity of Navs involves interaction with the actin-based cytoskeleton [9, 35], modulation of the VSD by the lipid surrounding [2], and interactions between  $\alpha$  and  $\beta$  subunits [17]. As  $\beta 1$  and  $\beta 3$  can also interact with actin-based cytoskeleton via different cytosolic proteins [18], these ability

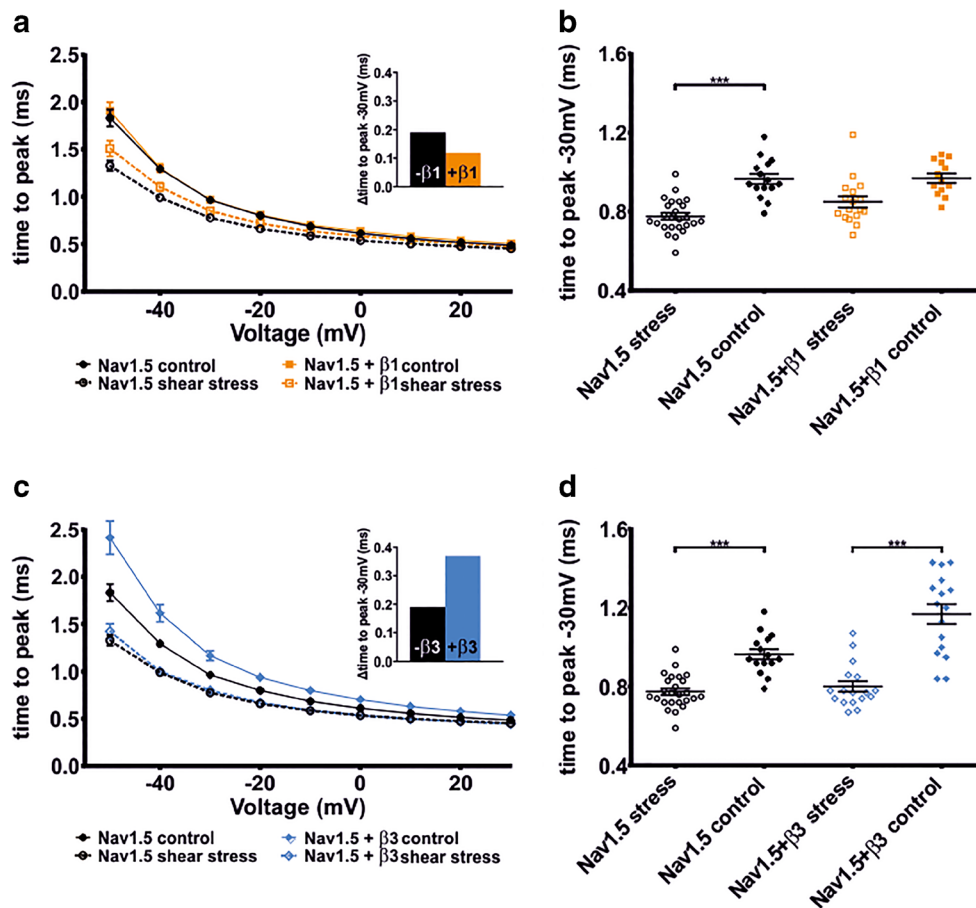


**Fig. 5**  $\beta 3$  expression enhances acceleration of activation kinetics of Nav1.5 by mechanical stress. Time to peak with and without mechanical stress was calculated for Nav1.5 alone and co-expressed with the  $\beta 1$  (a, b) or  $\beta 3$  subunit (c, d). **b, d** Statistical analysis for time to peak at  $-30$  mV where peak inward current was maximal. **a, b** Without stress  $\beta 1$  co-expression (Nav1.5 +  $\beta 1$  control, filled orange squares) did not affect time to peak when compared to Nav1.5 control (filled black circles). Mechanical stress decreased time to peak for both groups over the whole voltage range but did not reach significance for Nav1.5 +  $\beta 1$  at  $-30$  mV.  $\beta 1$  did not seem to alter the mechano-induced acceleration of activation and the difference of time to peak was similar in the absence (0.19 ms) and presence of  $\beta 1$  (0.12 ms, see also inset in a). Time to peak at  $-30$  mV is depicted for individual experiments and mean  $\pm$  SEM was

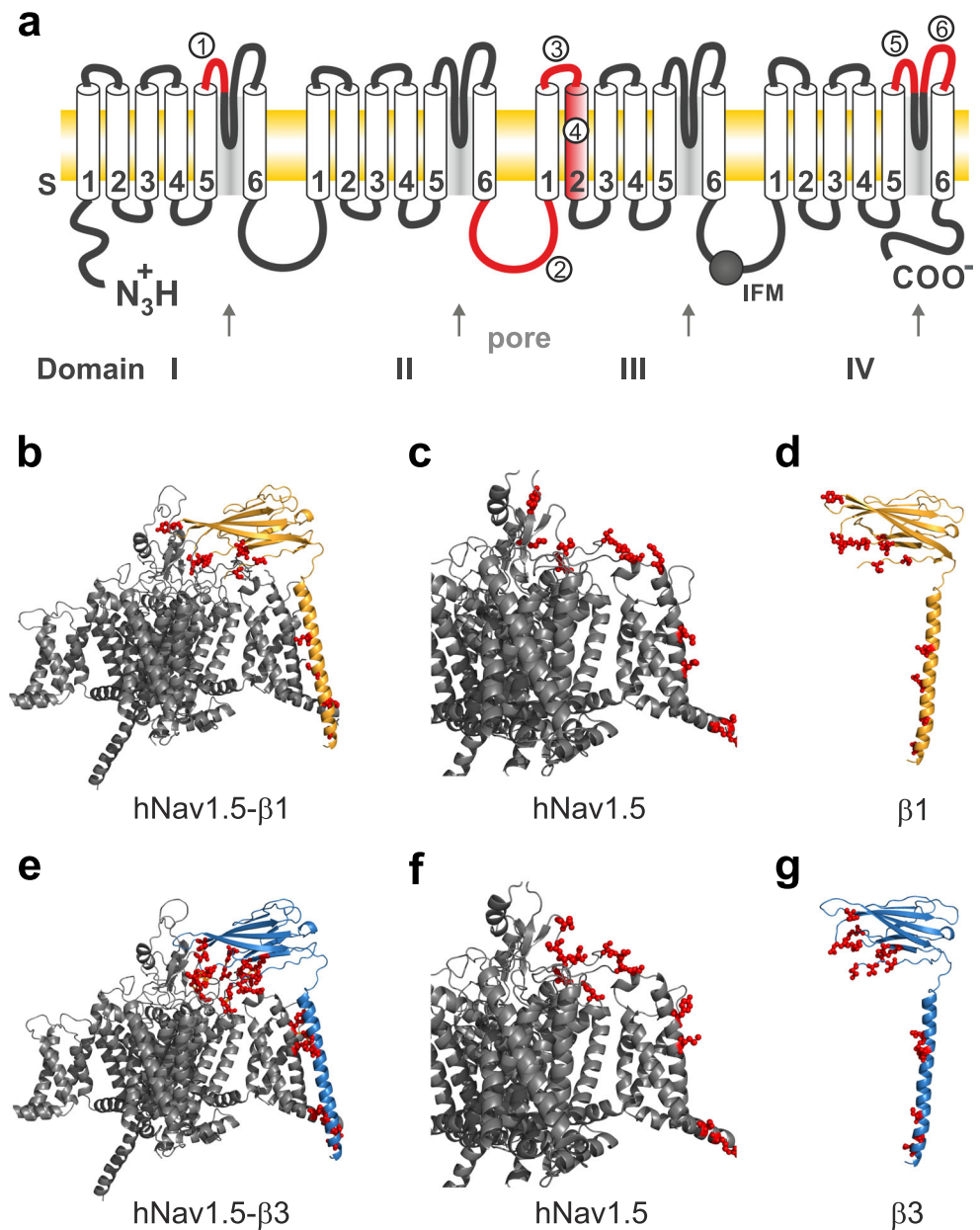
$0.97 \pm 0.03$  ms for Nav1.5 ( $n = 15$ ) and  $0.97 \pm 0.02$  ms for Nav1.5 +  $\beta 1$  ( $n = 13$ ) under control conditions. With mechanical stress time to peak was  $0.78 \pm 0.02$  ms for Nav1.5 ( $n = 25$ ) and  $0.85 \pm 0.03$  ms for Nav1.5 +  $\beta 1$  ( $n = 17$ ). **c, d** Without mechanical stress  $\beta 3$  co-expression showed a tendency to increase time to peak over the whole voltage range but did not reach significance at  $-30$  mV compared to Nav1.5 control. With mechanical stress activation kinetics for Nav1.5 and Nav1.5 +  $\beta 3$  were both accelerated but  $\beta 3$  almost doubled the  $\Delta$  time to peak which was 0.37 ms instead of 0.19 ms for Nav1.5 alone (inset in c). Mean values  $\pm$  SEM at  $-30$  mV were  $0.97 \pm 0.03$  ms for Nav1.5 control ( $n = 15$ ),  $1.17 \pm 0.05$  ms for Nav1.5 +  $\beta 3$  control ( $n = 16$ ),  $0.78 \pm 0.02$  ms for Nav1.5 stress ( $n = 25$ ) and  $0.8 \pm 0.03$  ms for Nav1.5 +  $\beta 3$  stress ( $n = 17$ ). Kruskal-Wallis ANOVA with Dunn's multiple comparison test

could be one explanation for their differential effects on mechanomodulation. The recently solved cryo-EM structures of the Nav1.4- $\beta 1$  complex from electric eel and man consistently showed that  $\beta 1$  is located close to the DIII VSD and interacts with extracellular loops of DI and DIV [27, 45]. Using a homology model, we found that  $\beta 3$  seems to have more interactions with DIII VSD and especially the extracellular parts of the pore loop domain IV. For  $\beta 1$  and Nav1.7, this region has been shown to be important for mechanostabilisation of inactivation as the C43A mutant of  $\beta 1$  that disturbs binding to the S5-S6 loop of DIV loses its ability to stabilise inactivation against mechanical stress but still selectively prevents the mechano-induced shifts in activation. Together with this observation, the stronger interactions of  $\beta 3$  with the extracellular

parts of S6DIV strengthen the evidence that this region might be especially important in mediating mechanomodulation of inactivation and could be an explanation why  $\beta 1$  co-expression is able to amplify mechano-induced shifts in inactivation whereas  $\beta 3$  is not.

However, homology modelling as indirect approach is limited by its assumption of a putative binding site as non-covalently  $\beta$  subunits have been shown to regulate gating of Nav1.5 via modulation of different VSDs [47]. The same group found non-additive effects for steady-state inactivation but cooperative effects for VSD-activation co-expressing Nav1.5 with  $\beta 1$  and  $\beta 3$  depending on interactions with different VSDs and also suggested that molecular level differences in  $\alpha$ - $\beta$  subunit interaction affect gating kinetics and

**Fig. 6** Scheme and homology model of Nav1.5 in complex with  $\beta 1$  and  $\beta 3$ . Schematic overview of the domains (DI-IV) and transmembrane segments (S1-6) of Nav1.5 (**a**). Interaction sites calculated by homology modelling with  $\beta 1$  and  $\beta 3$  are highlighted in red. Non-covalently bound  $\beta$  subunits were found to bind at the S5-PL-linker of DI (1), the S6 DII-S1 DIII-loop (2), the S1-S2-linker of DIII (3), S2 DIII (4), the S5-PL-linker of DIV (5) and the PL-S6-linker of DIV (6). PL: pore loop; IFM indicates the inactivation particle in the loop between DIII and DIV. Homology model of Nav1.5 in complex with the  $\beta 1$  (**b, c, d**) or  $\beta 3$  subunit (**e, f, g**) using the Nav1.4- $\beta 1$  complex from electric eel as template. Residues within a distance of 3 Å are shown as red spheres.  $\beta 3$  forms more interactions with Nav1.5 especially with VSDIII and the extracellular parts of the pore loop domain IV of Nav1.5



could promote binding to lower affinity binding sites. Based on our observation that  $\beta 3$  seems to share more interactions with Nav1.5 than  $\beta 1$ , it is tempting to speculate that if both  $\beta$  subunits would be able to bind to Nav1.5 at the same binding site, their modulatory effects could still be different due to unequal interactions with the extracellular loops of Navs. Furthermore, it might also be possible that a distinct  $\beta$  subunit isoform is not only able to interact with more than one binding site but also does not bind to the same binding site in all Nav isoforms. Our assumptions are further based on and match structural information of  $\alpha$ - $\beta$  complexes in which  $\beta$  subunits bind to the channel as a monomer [27, 33, 45]. However, there are studies that suggest Nav clustering by  $\beta$  subunits and trimerisation of  $\beta 3$  [19, 23, 24]. The interaction sites for

trimerisation however mostly overlap with those necessary for binding to the  $\alpha$  subunit. To address this question, further structural and functional studies are necessary to improve our understanding on how  $\beta$  subunits bind to and modulate Navs.

Implications for the contribution of mechanosensitivity of Navs1.5 in physiology and pathophysiology have been proposed for the cardiac electromechanical feedback [28] and have been strengthened by the observation that arrhythmia linked variants alter mechanomodulation of Nav1.5 [1]. Mutations affecting mechanosensitivity of Nav1.5 have recently also been linked to the pathophysiology of irritable bowel syndrome and mechanosensitive properties of Nav1.5 may be important for normal gastrointestinal motility [30, 37]. From those mutations or mutations in  $\beta 1$  and  $\beta 3$  associated

with arrhythmias known to date, none seem to directly affect any of the predicted binding sites in our homology model. However, our model suggests that Nav1.5 F1293S and Nav1.5 S1770G [34, 37],  $\beta 1$  D153N [43], and  $\beta 3$  V54G [39], A130V [41], and M161T [15, 26] are localised in close proximity of some of the predicted interaction sites. Therefore, it is tempting to speculate that these mutations might interfere with the mechanoregulation of Nav1.5 by  $\beta 1$  and  $\beta 3$  and indicate a potential involvement of  $\beta$  subunits in the pathology of irritable bowel syndrome. However, further studies are necessary to elucidate this issue in more detail.

Recently, mechanomodulation of Nav1.7 has been discovered as new property of the regulatory  $\beta 1$  subunit. In this study, the regulation of mechanosensitivity of the cardiac sodium channel Nav1.5 by the non-covalently bound  $\beta$  subunits  $\beta 1$  and  $\beta 3$  has been investigated. In summary, our findings indicate that mechanomodulation is not a property unique to  $\beta 1$  and seems to differ between distinct Nav  $\alpha$  and  $\beta$  isoforms.  $\beta 1$  and  $\beta 3$  differentially regulated mechanosensitivity of Nav1.5 and we describe an enhancement of mechano-induced acceleration of gating kinetics as novel mechanism of mechanomodulation. Our data provide further insights into the antiarrhythmogenic action of  $\beta$  subunits and strengthen the evidence that mechanosensitivity seems to be an accurately regulated property of Navs that possesses potential pathological and pharmacological implications

**Acknowledgements** We thank Daniela Graef, Brigitte Hoch, and Petra Hautvast for the excellent technical support, Martin Hampl for the advice on analysis of patch clamp data and Professor Christian Alzheimer and PD Tobias Huth for the use of laboratory facilities.

**Author contribution** MM: performed patch-clamp experiments, analysed and interpreted the data, contributed to the manuscript

JK: performed homology modelling, analysed, interpreted and discussed the data, reviewed the manuscript

JS: conceived the study, reviewed the manuscript

BW: conceived the study, discussed the data, reviewed the manuscript

AL: conceived the study, interpreted and discussed the data, reviewed the manuscript

EE: conceived the study, planned experiments, analysed and interpreted the data, wrote the manuscript

**Funding** None of the mentioned funding sources were involved in the study design, data collection and analysis, interpretation of the data, writing the paper or decision to submit the paper for publication.

This work was supported by the Interdisciplinary Center for Clinical Research (University Hospital Erlangen, IZKF projects E25 and Junior Project J66 and rotation fellowship to EE) the German Federal Ministry of Education and Research (BMBF 01EK1609A), the German Research Foundation (DFG RTG 2162, RTG 2416, LA 2740/3-1), the Bavarian Ministry of Science, and the Arts in the framework of ForInter.

**Data availability** The datasets analysed during the current study are available from the corresponding author on reasonable request.

## Compliance with ethical standards

**Conflict of interest** The authors declare that they have no conflict of interest.

**Ethical approval** This article does not contain any studies with human participants or animals performed by any of the authors.

## References

- Banderali U, Juranka PF, Clark RB, Giles WR, Morris CE (2010) Impaired stretch modulation in potentially lethal cardiac sodium channel mutants. *Channels (Austin)* 4:12–21
- Beyder A, Rae JL, Bernard C, Strege PR, Sachs F, Farrugia G (2010) Mechanosensitivity of Nav1.5, a voltage-sensitive sodium channel. *J Physiol* 588:4969–4985. <https://doi.org/10.1113/jphysiol.2010.199034>
- Beyder A, Strege PR, Bernard C, Farrugia G (2012) Membrane permeable local anesthetics modulate Na(V)1.5 mechanosensitivity. *Channels (Austin)* 6:308–316. <https://doi.org/10.4161/chan.21202>
- Beyder A, Strege PR, Reyes S, Bernard CE, Terzic A, Makielski J, Ackerman MJ, Farrugia G (2012) Ranolazine decreases mechanosensitivity of the voltage-gated sodium ion channel Na(v)1.5: a novel mechanism of drug action. *Circulation* 125: 2698–2706. <https://doi.org/10.1161/CIRCULATIONAHA.112.094714>
- Blanchard MG, Willemsen MH, Walker JB, Dib-Hajj SD, Waxman SG, Jongmans MC, Kleefstra T, van de Warrenburg BP, Praamstra P, Nicolai J, Yntema HG, Bindels RJ, Meisler MH, Kamsteeg EJ (2015) De novo gain-of-function and loss-of-function mutations of SCN8A in patients with intellectual disabilities and epilepsy. *J Med Genet*. <https://doi.org/10.1136/jmedgenet-2014-102813>
- Brackenbury WJ, Isom LL (2011) Na channel  $\beta$  subunits: over-achievers of the ion channel family. *Front Pharmacol* 2:53. <https://doi.org/10.3389/fphar.2011.00053>
- Catterall WA (2012) Voltage-gated sodium channels at 60: structure, function and pathophysiology. *J Physiol* 590:2577–2589. <https://doi.org/10.1113/jphysiol.2011.224204>
- Catterall WA, Goldin AL, Waxman SG (2005) International Union of Pharmacology. XLVII. Nomenclature and structure-function relationships of voltage-gated sodium channels. *Pharmacol Rev* 57: 397–409. <https://doi.org/10.1124/pr.57.4.4>
- Chahine M, Ziane R, Vijayaragavan K, Okamura Y (2005) Regulation of Na<sup>v</sup> channels in sensory neurons. *Trends Pharmacol Sci* 26:496–502. <https://doi.org/10.1016/j.tips.2005.08.002>
- Chen C, Westenbroek RE, Xu X, Edwards CA, Sorenson DR, Chen Y, McEwen DP, O'Malley HA, Bharucha V, Meadows LS, Knudsen GA, Vilaythong A, Noebels JL, Saunders TL, Scheuer T, Shrager P, Catterall WA, Isom LL (2004) Mice lacking sodium channel beta1 subunits display defects in neuronal excitability, sodium channel expression, and nodal architecture. *J Neurosci* 24: 4030–4042. <https://doi.org/10.1523/JNEUROSCI.4139-03.2004>
- Edokobi N, Isom LL (2018) Voltage-gated sodium channel  $\beta 1/\beta 1B$  subunits regulate cardiac physiology and pathophysiology. *Front Physiol* 9:351. <https://doi.org/10.3389/fphys.2018.00351>
- Grant AO (2009) Cardiac ion channels. *Circ Arrhythm Electrophysiol* 2:185–194. <https://doi.org/10.1161/CIRCEP.108.789081>
- Hakim P, Brice N, Thresher R, Lawrence J, Zhang Y, Jackson AP, Grace AA, Huang CL-H (2010) *Scn3b* knockout mice exhibit abnormal sino-atrial and cardiac conduction properties. *Acta Physiol*

- (Oxford) 198:47–59. <https://doi.org/10.1111/j.1748-1716.2009.02048.x>
14. Hu D, Barajas-Martinez H, Burashnikov E, Springer M, Wu Y, Varro A, Pfeiffer R, Koopmann TT, Cordeiro JM, Guerchicoff A, Pollevick GD, Antzelevitch C (2009) A mutation in the beta 3 subunit of the cardiac sodium channel associated with Brugada ECG phenotype. *Circ Cardiovasc Genet* 2:270–278. <https://doi.org/10.1161/CIRCGENETICS.108.829192>
  15. Ishikawa T, Takahashi N, Ohno S, Sakurada H, Nakamura K, On YK, Park JE, Makiyama T, Horie M, Arimura T, Makita N, Kimura A (2013) Novel SCN3B mutation associated with brugada syndrome affects intracellular trafficking and function of Nav1.5. *Circ J* 77:959–967. <https://doi.org/10.1253/circj.CJ-12-0995>
  16. Kaufmann SG, Westenbroek RE, Maass AH, Lange V, Renner A, Wischmeyer E, Bonz A, Muck J, Ertl G, Catterall WA, Scheuer T, Maier SKG (2013) Distribution and function of sodium channel subtypes in human atrial myocardium. *J Mol Cell Cardiol* 61:133–141. <https://doi.org/10.1016/j.yjmcc.2013.05.006>
  17. Kömer J, Meents J, Machtens J-P, Lampert A (2018)  $\beta$ 1 subunit stabilises sodium channel Nav1.7 against mechanical stress. *J Physiol* 596:2433–2445. <https://doi.org/10.1113/JP275905>
  18. McEwen DP, Chen C, Meadows LS, Lopez-Santiago L, Isom LL (2009) The voltage-gated Na<sup>+</sup> channel beta3 subunit does not mediate trans homophilic cell adhesion or associate with the cell adhesion molecule contactin. *Neurosci Lett* 462:272–275. <https://doi.org/10.1016/j.neulet.2009.07.020>
  19. Mercier A, Clément R, Hamois T, Bourmeyster N, Faivre J-F, Findlay I, Chahine M, Bois P, Chatelier A (2012) The  $\beta$ 1-subunit of Na(v)1.5 cardiac sodium channel is required for a dominant negative effect through  $\alpha$ - $\alpha$  interaction. *PLoS One* 7:e48690. <https://doi.org/10.1371/journal.pone.0048690>
  20. Moreno JD, Clancy CE (2012) Pathophysiology of the cardiac late Na current and its potential as a drug target. *J Mol Cell Cardiol* 52:608–619. <https://doi.org/10.1016/j.yjmcc.2011.12.003>
  21. Morris CE (2011) Voltage-gated channel mechanosensitivity: fact or friction? *Front Physiol* 2:25. <https://doi.org/10.3389/fphys.2011.00025>
  22. Morris CE, Juranka PF (2007) Nav channel mechanosensitivity: activation and inactivation accelerate reversibly with stretch. *Biophys J* 93:822–833. <https://doi.org/10.1529/biophysj.106.101246>
  23. Namadurai S, Balasuriya D, Rajappa R, Wiemhöfer M, Stott K, Klingauf J, Edwardson JM, Chirgadze DY, Jackson AP (2014) Crystal structure and molecular imaging of the Nav channel  $\beta$ 3 subunit indicates a trimeric assembly. *J Biol Chem* 289:10797–10811. <https://doi.org/10.1074/jbc.M113.527994>
  24. Namadurai S, Yereddi NR, Cusdin FS, Huang CLH, Chirgadze DY, Jackson AP (2015) A new look at sodium channel  $\beta$  subunits. *Open Biol* 5:140192. <https://doi.org/10.1098/rsob.140192>
  25. O'Malley HA, Isom LL (2015) Sodium channel  $\beta$  subunits: emerging targets in channelopathies. *Annu Rev Physiol* 77:481–504. <https://doi.org/10.1146/annurev-physiol-021014-071846>
  26. Olesen MS, Jespersen T, Nielsen JB, Liang B, Møller DV, Hedley P, Christiansen M, Varró A, Olesen S-P, Haunsø S, Schmitt N, Svendsen JH (2011) Mutations in sodium channel  $\beta$ -subunit SCN3B are associated with early-onset lone atrial fibrillation. *Cardiovasc Res* 89:786–793. <https://doi.org/10.1093/cvr/cvq348>
  27. Pan X, Li Z, Zhou Q, Shen H, Wu K, Huang X, Chen J, Zhang J, Zhu X, Lei J, Xiong W, Gong H, Xiao B, Yan N (2018) Structure of the human voltage-gated sodium channel Nav1.4 in complex with  $\beta$ 1. *Science*:362. <https://doi.org/10.1126/science.aau2486>
  28. Peyronnet R, Nerbonne JM, Kohl P (2016) Cardiac mechano-gated ion channels and arrhythmias. *Circ Res* 118:311–329. <https://doi.org/10.1161/CIRCRESAHA.115.305043>
  29. Rush AM, Cummins TR, Waxman SG (2007) Multiple sodium channels and their roles in electrogenesis within dorsal root ganglion neurons. *J Physiol* 579:1–14. <https://doi.org/10.1113/jphysiol.2006.121483>
  30. Saito YA, Strege PR, Tester DJ, Locke GR, Talley NJ, Bernard CE, Rae JL, Makielski JC, Ackerman MJ, Farrugia G (2009) Sodium channel mutation in irritable bowel syndrome: evidence for an ion channelopathy. *Am J Physiol Gastrointest Liver Physiol* 296:G211–G218. <https://doi.org/10.1152/ajpgi.90571.2008>
  31. Sali A, Blundell TL (1993) Comparative protein modelling by satisfaction of spatial restraints. *J Mol Biol* 234:779–815. <https://doi.org/10.1006/jmbi.1993.1626>
  32. Shcherbatko A, Ono F, Mandel G, Brehm P (1999) Voltage-dependent sodium channel function is regulated through membrane mechanics. *Biophys J* 77:1945–1959. [https://doi.org/10.1016/S0006-3495\(99\)77036-0](https://doi.org/10.1016/S0006-3495(99)77036-0)
  33. Shen H, Liu D, Wu K, Lei J, Yan N (2019) Structures of human Nav1.7 channel in complex with auxiliary subunits and animal toxins. *Science* 363:1303–1308. <https://doi.org/10.1126/science.aaw2493>
  34. Sommariva E, Vatta M, Xi Y, Sala S, Ai T, Cheng J, Pappone C, Ferrari M, Benedetti S (2012) Compound heterozygous SCN5A gene mutations in asymptomatic Brugada syndrome child. *Cardiogenetics* 2:11. <https://doi.org/10.4081/cardiogenetics.2012.e11>
  35. Strege PR, Holm AN, Rich A, Miller SM, Ou Y, Sarr MG, Farrugia G (2003) Cytoskeletal modulation of sodium current in human jejunal circular smooth muscle cells. *Am J Physiol Cell Physiol* 284:C60–C66. <https://doi.org/10.1152/ajpcell.00532.2001>
  36. Strege P, Beyder A, Bernard C, Crespo-Diaz R, Behfar A, Terzic A, Ackerman M, Farrugia G (2012) Ranolazine inhibits shear sensitivity of endogenous Na<sup>+</sup> current and spontaneous action potentials in HL-1 cells. *Channels (Austin)* 6:457–462. <https://doi.org/10.4161/chan.22017>
  37. Strege PR, Mazzone A, Bernard CE, Neshatian L, Gibbons SJ, Saito YA, Tester DJ, Calvert ML, Mayer EA, Chang L, Ackerman MJ, Beyder A, Farrugia G (2018) Irritable bowel syndrome patients have SCN5A channelopathies that lead to decreased Nav1.5 current and mechanosensitivity. *Am J Physiol Gastrointest Liver Physiol* 314:G494–G503. <https://doi.org/10.1152/ajpgi.00016.2017>
  38. Tabarean IV, Juranka P, Morris CE (1999) Membrane stretch affects gating modes of a skeletal muscle sodium channel. *Biophys J* 77:758–774. [https://doi.org/10.1016/S0006-3495\(99\)76930-4](https://doi.org/10.1016/S0006-3495(99)76930-4)
  39. Valdivia CR, Medeiros-Domingo A, Ye B, Shen W-K, Algiers TJ, Ackerman MJ, Makielski JC (2010) Loss-of-function mutation of the SCN3B-encoded sodium channel  $\beta$ 3 subunit associated with a case of idiopathic ventricular fibrillation. *Cardiovasc Res* 86:392–400. <https://doi.org/10.1093/cvr/cvp417>
  40. Wang JA, Lin W, Morris T, Banderali U, Juranka PF, Morris CE (2009) Membrane trauma and Na<sup>+</sup> leak from Nav1.6 channels. *Am J Physiol Cell Physiol* 297:C823–C834. <https://doi.org/10.1152/ajpcell.00505.2008>
  41. Wang P, Yang Q, Wu X, Yang Y, Shi L, Wang C, Wu G, Xia Y, Yang B, Zhang R, Xu C, Cheng X, Li S, Zhao Y, Fu F, Liao Y, Fang F, Chen Q, Tu X, Wang QK (2010) Functional dominant-negative mutation of sodium channel subunit gene SCN3B associated with atrial fibrillation in a Chinese GeneID population. *Biochem Biophys Res Commun* 398:98–104. <https://doi.org/10.1016/j.bbrc.2010.06.042>
  42. Watanabe H, Koopmann TT, Le Scouarnec S, Yang T, Ingram CR, Schott J-J, Demolombe S, Probst V, Anselme F, Escande D, Wiesel ACP, Pfeufer A, Kääh S, Wichmann H-E, Hasdemir C, Aizawa Y, Wilde AAM, Roden DM, Bezzina CR (2008) Sodium channel  $\beta$ 1 subunit mutations associated with Brugada syndrome and cardiac conduction disease in humans. *J Clin Invest* 118:2260–2268. <https://doi.org/10.1172/JCI33891>

43. Watanabe H, Darbar D, Kaiser DW, Jiramongkolchai K, Chopra S, Donahue BS, Kannankeril PJ, Roden DM (2009) Mutations in sodium channel  $\beta$ 1- and  $\beta$ 2-subunits associated with atrial fibrillation. *Circ Arrhythm Electrophysiol* 2:268–275. <https://doi.org/10.1161/CIRCEP.108.779181>
44. Waterhouse AM, Procter JB, Martin DMA, Clamp M, Barton GJ (2009) Jalview Version 2—a multiple sequence alignment editor and analysis workbench. *Bioinformatics* 25:1189–1191. <https://doi.org/10.1093/bioinformatics/btp033>
45. Yan Z, Zhou Q, Wang L, Wu J, Zhao Y, Huang G, Peng W, Shen H, Lei J, Yan N (2017) Structure of the Nav1.4- $\beta$ 1 complex from electric eel. *Cell* 170:470–482.e11. <https://doi.org/10.1016/j.cell.2017.06.039>
46. Zhang Z, Schmelz M, Segerdahl M, Quiding H, Centerholt C, Juréus A, Carr TH, Whiteley J, Salter H, Kvernebo MS, Ørstavik K, Helås T, Kleggetveit I-P, Lunden LK, Jørum E (2014) Exonic mutations in SCN9A (Nav1.7) are found in a minority of patients with erythromelalgia. *Scand J Pain* 5:217–225. <https://doi.org/10.1016/j.sjpain.2014.09.002>
47. Zhu W, Voelker TL, Varga Z, Schubert AR, Nerbonne JM, Silva JR (2017) Mechanisms of noncovalent  $\beta$  subunit regulation of Nav channel gating. *J Gen Physiol*. <https://doi.org/10.1085/jgp.201711802>
48. Zimmer T, Biskup C, Bollensdorff C, Benndorf K (2002) The beta1 subunit but not the beta2 subunit colocalizes with the human heart Na<sup>+</sup> channel (hH1) already within the endoplasmic reticulum. *J Membr Biol* 186:13–21. <https://doi.org/10.1007/s00232-001-0131-0>

**Publisher's note** Springer Nature remains neutral with regard to jurisdictional claims in published maps and institutional affiliations.